

4-3-2014


Learning Two-input Linear and Nonlinear Analog Functions with a Simple Chemical System

Peter Banda
Portland State University

Christof Teuscher
Portland State University, teuscher@pdx.edu

Let us know how access to this document benefits you.

Follow this and additional works at: https://pdxscholar.library.pdx.edu/compsci_fac

 Part of the [Artificial Intelligence and Robotics Commons](#), and the [Other Computer Sciences Commons](#)

Citation Details

Banda, Peter, and Christof Teuscher. "Learning Two-input Linear and Nonlinear Analog Functions with a Simple Chemical System."
arXiv preprint arXiv:1404.0427 (2014)

This Pre-Print is brought to you for free and open access. It has been accepted for inclusion in Computer Science Faculty Publications and Presentations by an authorized administrator of PDXScholar. For more information, please contact pdxscholar@pdx.edu.

Learning Two-input Linear and Nonlinear Analog Functions with a Simple Chemical System

Peter Banda*¹ and Christof Teuscher†²

¹Department of Computer Science, Portland State University

²Department of Electrical and Computer Engineering, Portland State University

April 3, 2014

Abstract

The current biochemical information processing systems behave in a pre-determined manner because all features are defined during the design phase. To make such unconventional computing systems reusable and programmable for biomedical applications, adaptation, learning, and self-modification based on external stimuli would be highly desirable. However, so far, it has been too challenging to implement these in real or simulated chemistries. In this paper we extend the chemical perceptron, a model previously proposed by the authors, to function as an analog instead of a binary system. The new analog asymmetric signal perceptron learns through feedback and supports Michaelis-Menten kinetics. The results show that our perceptron is able to learn linear and nonlinear (quadratic) functions of two inputs. To the best of our knowledge, it is the first simulated chemical system capable of doing so. The small number of species and reactions allows for a mapping to an actual wet implementation using DNA-strand displacement or deoxyribozymes. Our results are an important step toward actual biochemical systems that can learn and adapt.

Keywords

chemical perceptron, analog perceptron, supervised learning, chemical computing, RNMSE, linear function, quadratic function

1 Introduction

Biochemical information processing systems, which are crucial for emerging biomedical applications, cannot typically be programmed once built. After an *in vitro* or *in vivo* injection, the behavior, i.e., the program of such nano-scale chemical machines

*banda@pdx.edu

†teuscher@pdx.edu

[1] cannot be changed. That limits their applicability and re-usability. To address this limitation, future biochemical machinery should function not only in uniform, well-known lab settings but also in previously unknown environments. Such adaptive chemical systems would decide autonomously and learn new behaviors through reinforcements in response to external stimuli. We could imagine that in the future millions of molecular spiders [2] would help our immune system fight viruses, deliver medications [3], or fix broken cells. Adaptive chemical systems may also simplify the manufacturing and design processes: instead of designing multiple systems with predefined functionality embedded in their species and reactions one could train and recycle a single adaptive machine for a desired functionality.

Neural network theory [4] inspired numerous chemical implementations [5, 6, 7], however, only the input-weight integration part of a single perceptron model [8] was successfully mapped to chemistry. Learning (i.e., weight adaptation) was either not addressed or delegated to an external non-chemical system [7, 9] that calculated new weights values (i.e., chemical concentrations) to achieve a desired system behavior.

Our previous work [10] introduced the first simulated chemical system that can learn and adapt autonomously to feedback provided by a teacher. We coined the term *chemical perceptron* because the system qualitatively mimics a two-input binary perceptron. In a second step we aimed to simplify the model to make wet biochemical implementations feasible. We achieved that by employing the asymmetric representation of values and by using thresholding. The new *asymmetric signal perceptron* (ASP) model [11] requires less than a half of the reactions of its predecessors with comparable performance (i.e., 99.3 – 99.99% success rates). The flip side of the more compact design is a reduced robustness to rate constant perturbations due to a lack of structural redundancy.

In real biomedical applications one is often required to distinguish subtle changes in concentrations with complex linear or nonlinear relations among species. Such behavior cannot easily be achieved with our previous binary perceptron models, thus, several improvements are necessary. In this paper we present a new *analog asymmetric signal perceptron* (AASP) with two inputs. We will refer to the original ASP as a binary ASP (BASP). The AASP model follows mass-action and Michaelis-Menten kinetics and learns through feedback from the environment. The design is modular and extensible to any number of inputs. We demonstrate that the AASP can learn various linear and nonlinear functions. For example, it is possible to learn to produce the average of two analog values. In combination with a chemical delay line [12], the AASP could also be used to predict time series.

2 Chemical Reaction Network

To model the AASP we employ the *chemical reaction network* (CRN) formalism. A CRN consists of a finite set of molecular species and reactions paired with rate constants [13]. CRN represents an unstructured macroscopic simulated chemistry, hence, the species labeled with symbols are not assigned a molecular structure yet. More importantly, since the reaction tank is assumed to be well-stirred, CRN lacks the notion of space. The state of the system does therefore not contain any spatial

information and is effectively reduced to a vector of species concentrations. Without losing generality we treat a concentration as a dimensionless quantity. Depending on the required scale, a wet chemical implementation could use $\text{mol} \cdot \text{L}^{-1}$ (M) or $\text{nanomol} \cdot \text{L}^{-1}$ (nM) with appropriate (scaled) rate constant units, such as $M \cdot \text{s}^{-1}$ or $M^{-1} \cdot \text{s}^{-1}$, depending on the order of a reaction.

The reaction rate defines the speed of a reaction application prescribed by kinetic laws. The mass-action law [13] states that the rate of a reaction is proportional to the product of the concentrations of the reactants. For an irreversible reaction $aS_1 + bS_2 \rightarrow P$, the rate is given by

$$r = \frac{d[P]}{dt} = -\frac{1}{a} \frac{d[S_1]}{dt} = -\frac{1}{b} \frac{d[S_2]}{dt} = k[S_1]^a[S_2]^b,$$

where $k \in \mathbb{R}^+$ is a reaction rate constant, a and b are stoichiometric constants, $[S_1]$ and $[S_2]$ are concentrations of reactants (substrates) S_1 and S_2 , and $[P]$ is a concentration of product P .

Michaelis-Menten enzyme kinetics [14] describes the rate of a catalytic reaction $E + S \rightleftharpoons ES \rightarrow E + P$, where a substrate S transforms to a product P with a catalyst E , which increases the rate of a reaction without being altered. A species ES is an intermediate enzyme-substrate binding. By assuming quasi-steady-state approximation, the rate is given by

$$r = \frac{d[P]}{dt} = \frac{k_{cat}[E][S]}{K_m + [S]},$$

where $k_{cat}, K_m \in \mathbb{R}^+$ are rate constants. By combining kinetic expressions for all species, we obtain a system of ODEs that we simulate using 0.1-step Runge-Kutta4 numerical integration.

3 Model

The AASP models a formal analog perceptron [8] with two inputs x_1 and x_2 , similar to an early type of artificial neuron [4]. The perceptron is capable of simple learning and can be used as a building block of a feed-forward neural networks. Networks built from perceptrons have been shown to be universal approximators [15].

In a CRN we represent each formal variable with one or several species. While the previous BASP models a perceptron with two inputs and a binary output produced by external or internal thresholding, the new AASP is analog and does not use thresholding. Instead of a binary yes/no answer, its output is analog, which requires much finer control over the weight convergence. As a consequence, the AASP consists of more species, namely 17 vs. 13, and more reactions, namely 18 vs. 16.

3.1 Input-Weight Integration

A formal perceptron integrates the inputs \mathbf{x} with the weights \mathbf{w} linearly as $\sum_{i=0}^n w_i \cdot x_i$, where the weight w_0 , a bias, always contributes to an output because its associated

Table 1: (a) The AASP’s species divided into groups according to their purpose and functional characteristics; (b) the AASP’s reactions with the best rate constants found by the GA (see Section 3.3), rounded to four decimals. Groups 1 – 4 implement the input-weight integrations, the rest implement learning.

Group Name	Species	Group	Reaction	Catalyst	Rates
Inputs	X_1, X_2	1	$S_{in} + Y \rightarrow \lambda$.1800
Output	Y	2	$S_{in} \rightarrow Y + S_{in}Y$	W_0	.5521, 2.5336
Weights	W_0, W_1, W_2	3	$X_1 + Y \rightarrow \lambda$ $X_2 + Y \rightarrow \lambda$.3905
Target output	\hat{Y}	4	$X_1 \rightarrow Y + X_1Y$ $X_2 \rightarrow Y + X_2Y$	W_1 W_2	.4358, 0.1227
Input (clock) signal	S_{in}	5	$\hat{Y} \rightarrow W^\oplus$.1884
Learning signal	S_L	6	$Y \rightarrow W^\ominus$	S_L	.1155, 1.9613
Input contributions	$X_1Y, X_2Y, S_{in}Y$	7	$Y + \hat{Y} \rightarrow \lambda$		1.0000
Weight changers	$W^\ominus, W^\oplus,$ $W_0^\ominus, W_1^\ominus, W_2^\ominus$	8	$W^\ominus \rightarrow W_0^\ominus$	$S_{in}Y$	0.600, 1.6697
Total	17	9	$W_0 + W_0^\ominus \rightarrow \lambda$.2642
		10	$W^\oplus \rightarrow W_0$	$S_{in}Y$.5023, 2.9078
		11	$W^\ominus \rightarrow W_1^\ominus$ $W^\ominus \rightarrow W_2^\ominus$	X_1Y X_2Y	.1889, 1.6788
		12	$W_1 + W_1^\ominus \rightarrow \lambda$ $W_2 + W_2^\ominus \rightarrow \lambda$.2416
		13	$W^\oplus \rightarrow W_1$ $W^\oplus \rightarrow W_2$	X_1Y X_2Y	.2744, 5.0000
		Total		18	

input $x_0 = 1$. An activation function φ , such as a hyperbolic tangent or sigmoid, then processes the dot product to produce the output y .

The reactions carrying out the chemical input-weight integration are structurally the same as in the BASP. The only difference is an addition of the partial input-weight contribution species, which are, however, required for learning only, and will be explained in Section 3.1. The AASP models a two-input perceptron where the output calculation is reduced to $y = \varphi(w_0 + w_1x_1 + x_2w_2)$. The concentration of input species X_1 and X_2 corresponds to the formal inputs x_1 and x_2 , and the species Y to the output y . A clock (input) signal S_{in} is always provided along the regular input X_1 and X_2 , since it serves as the constant-one coefficient (or the constant input $x_0 = 1$) of the bias weight w_0 .

The AASP represents the weights by three species W_1, W_2 , and W_0 . As opposed to the formal model, the input-weight integration is nonlinear and based on an annihilatory version of the asymmetric representation of the values and the addition/subtraction operation as introduced in [11]. Since the concentration cannot be negative, we cannot map a signed real variable directly to the concentration of a single species. The weights require both positive and negative values, otherwise we could cover only functions that are strictly additive. The asymmetric representation uses a single species E that catalyzes a transformation of substrate S to a product P ($S \xrightarrow{E} P$) and competes against an annihilation of the substrate and the product $S + P \rightarrow \lambda$. For a given threshold concentration of the product we can determine the associated catalyst threshold, so all concentrations of catalyst $[E]_0$ to the left

of this threshold represent negative numbers while all concentrations to the right represent positive numbers. The final product concentration $[P]_\infty$ is monotonically increasing and asymptotically reaches the initial concentration of the substrate $[S]_0$ for $[E]_0 \rightarrow \infty$.

Using the asymmetric comparison primitives, we map the AASP's weights to catalysts (E), the inputs to substrates (S), and the output to product (P) and obtain 6 reactions as shown in Figure 1(a) and Table 1(b), groups 1 – 4. Each weight species races with its substrate's annihilation but also with other weights. Since the output Y is shared, this effectively implements a nonlinear input-weight integration. Note that by replacing annihilation with a decay of input species, we would end up having three independent races with additive contributions instead of one global race. An alternative symmetric representation embedded in the former *weight-loop perceptron* and the *weight-race perceptron* [10] encodes the values by two complementary species, one for the positive and one for the negative domain. We opt for the asymmetric approach because it reduces the number of reactions by half compared to the symmetric one.

Because of the complexity of the underlying ODEs, no closed formula for the output concentration exists and theoretical conclusions are very limited. Although we cannot analyze the input-weight integration dynamics quantitatively, we can still describe the qualitative behavior and constraints. The weight concentration represents formally both positive and negative values, so the weights together with annihilatory reactions can act as both catalysts and inhibitors. More specifically a low weight concentration, which strengthens its input-specific annihilation, could impose a negative pressure on a different weight branch. Hence, we interpret a weight that contributes to the output less than its input consumes as negative. In an extreme case, when the weight concentration is zero, its branch would consume the same amount of output as its input injected. The relation between the concentration of weights and the final output $[Y]_\infty$ has a sigmoidal shape with the limit $[X_1]_0 + [X_2]_0 + [S_{in}]_0$ reaching for all weights $[W_i] \rightarrow \infty$. Clearly the output concentration cannot exceed all the inputs provided.

Figure 2 shows the relation between the concentration of weight W_1 and weight W_2 and the final output concentration. For simplicity the bias processing part is not considered ($[S_{in}] = 0$), so we keep only two branches of the input-weight integration triangle. Note that in the plots the concentration of weights span the interval 0 to 2 because in our simulations we draw the weights uniformly from the interval (0.5, 1.5). On the z-axis we plotted the ratio of the output concentration $[Y]$ to $[X_1]_0 + [X_2]_0$. For learning to work we want the gradient of the output surface to be responsive to changes in the weight concentrations. Therefore, we restrict the range of possible outputs so it is neither too close to the maximal output, where the surface is effectively constant, nor too close to zero, where the surface is too steep and even a very small perturbation of the weight concentration would dramatically change the output.

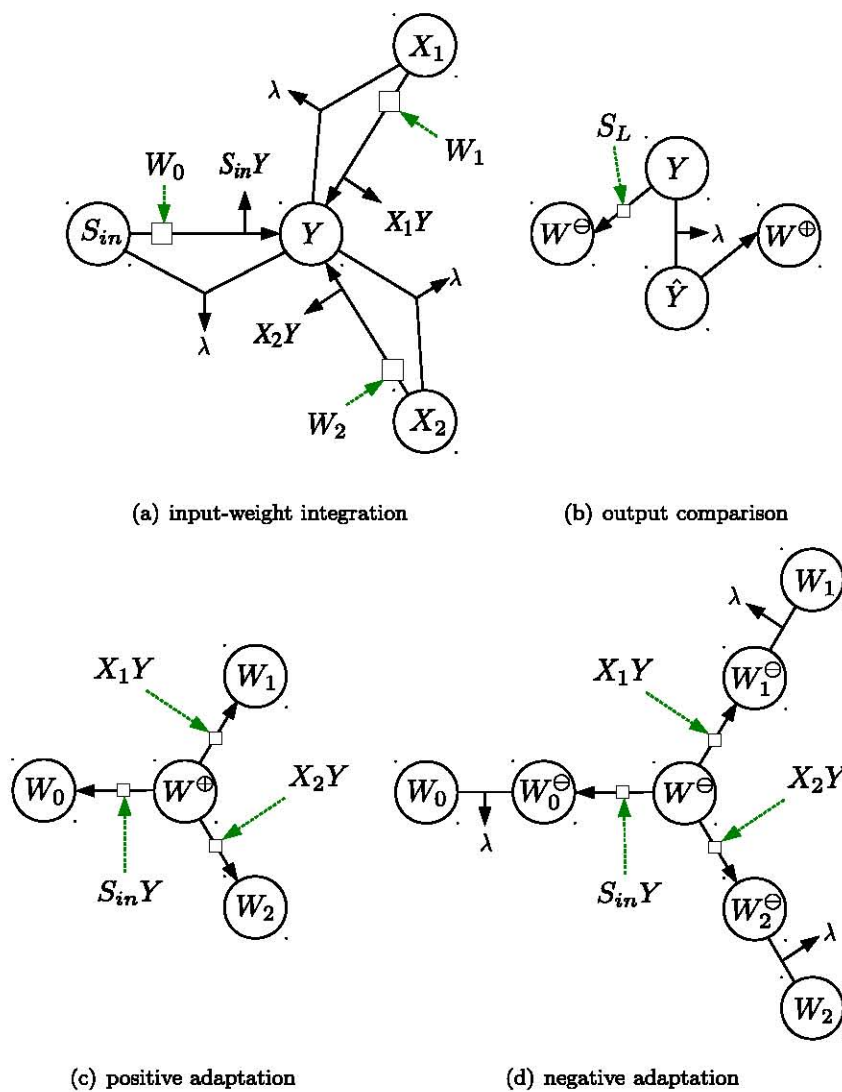


Figure 1: (a) The AASP's reactions performing input-weight integration. Similarly to the BASP, cross-weight competition is achieved by the annihilation of the inputs S_{in} , X_1 , X_2 with the output Y , an asymmetric strategy for representation of real values and subtraction. (b-d) the AASP's reactions responsible for learning. They are decomposed into three parts: (b) comparison of the output Y with the target-output \hat{Y} , determining whether weights should be incremented (W^\oplus species) or decremented (W^\ominus species), and (c-d) positive and negative adaptation of the weights W_0 , W_1 , and W_2 , which is proportional to the part of the output they produced $S_{in}Y$, X_1Y , and X_2Y respectively. Nodes represent species, solid lines are reactions, dashed lines are catalysts, and λ stands for no or inert species.

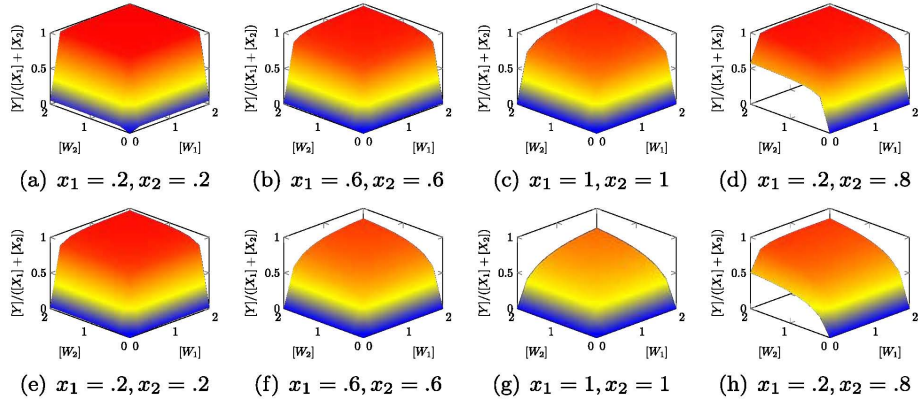


Figure 2: The relation between the weight concentrations $[W_1]$ and $[W_2]$ and the final output concentration $[Y]_\infty$ normalized by $[X_1]_0 + [X_2]_0$ for the input-weight integration (excluding the bias W_0 part) showing various inputs. The rate constant of annihilatory reactions $X_i + Y \rightarrow \lambda$, $i \in \{1, 2\}$ is $k = 0.2$ in the top and $k = 1$ in the bottom row.

3.2 Learning

In the previous BASP model learning reinforced the adaptation of weights by a penalty signal, whose presence indicated that the output was incorrect. Since the output is analog in the new AASP model, a simple penalty signal is not sufficient anymore. We therefore replaced the reinforcement learning by classical supervised learning [16]. Formally, the adaptation of a weight w_i for the training sample (\mathbf{x}, \hat{y}) , where \hat{y} is a target output, and \mathbf{x} a input vector, is defined as $\Delta w_i = \alpha(\hat{y} - y(t))x_i$, where $\alpha \in (0, 1]$ is the learning rate. The AASP's, similarly to the input-weight integration, does not implement the formal Δw_i adaptation precisely, rather, it follows the relation qualitatively.

The learning is triggered by an injection of the target output \hat{Y} provided some time after the injection of the input species. The part presented in Figure 1(b) compares the output Y and the target output \hat{Y} by annihilation. Intuitively a leftover of the regular output Y implies that the next time the AASP faces the same input, it must produce less output, and therefore it needs to decrease the weights by producing a negative weight changer W^\ominus from Y . In the opposite case, the AASP needs to increase the weights, hence \hat{Y} transforms to a positive weight changer W^\oplus . Since the AASP can produce output also without learning, just by the input-weight integration, we need to guard the reaction $Y \rightarrow W^\ominus$ by a learning signal S_L , which is injected with the target output and removed afterwards. To prevent creation of erroneous or premature weight changers, the annihilation $Y + \hat{Y} \rightarrow \lambda$ must be very rapid. Note that the difference between the actual output Y and the desired output \hat{Y} , materializing in the total concentration of weight changers W^\oplus and W^\ominus , must not be greater than the required weight adaptation, otherwise the weights would diverge. The learning rate α is therefore effectively incorporated in the concentration of W^\oplus and W^\ominus .

In the formal perceptron, the adaptation of a weight w_i is proportional to the current input x_i . Originally, the BASP distinguished which weights to adapt by a residual concentration of inputs X_1 and X_2 . Because the inputs as well as an adaptation decision were binary, we cared only about whether some of the unprocessed input were still left, but not about its precise concentration. Thus, an injection of the penalty signal could not happen too soon, neither too late. Because the AASP's learning needs more information, the input-weight integration introduced three additional species, namely the partial input-weight contributions X_1Y , X_2Y , $S_{in}Y$, which are produced alongside the regular output Y . A decision which weights to update based on the input-weight contributions could be made even after the input-weight integration is finished. That allows to postpone an injection of the target output \hat{Y} and the learning signal S_L .

Let us now cover a positive adaptation as shown in Figure 1(c), where the total amount of W^\oplus is distributed among participating weights. The input contribution species X_1Y , X_2Y , $S_{in}Y$ race over the substrate W^\oplus by catalyzing the reactions $W^\oplus \rightarrow W_i$, $i \in \{0, 1, 2\}$. Note that the traditional weight adaptation formula takes into account solely the input value, so here we depart further from the formal perceptron and have the combination of input and weights compete over W^\oplus . Since larger weights produce more output they get adapted more. In addition, once a weight reaches zero, it will not be recoverable.

The negative adaptation presented in Figure 1(d) is analogous to the positive one, but this time the input-weight contributions race over W^\ominus and produce intermediates W_0^\ominus , W_1^\ominus , W_2^\ominus , which annihilate with the weights. Again, because the magnitude of a weight update depends on the weight itself, this feedback loop protects the weight from falling too low and reaching zero (i.e., a point of no return). This is beneficial because as opposed to the formal perceptron, a weight value (concentration) cannot be physically negative.

To implement the entire learning algorithm, the AASP requires 12 reactions as presented in Table 1(b), groups 5 – 13.

3.3 Genetic Search

Since a manual trial-error setting of the rate constants would be very time-consuming, we optimize the rate constants by a standard genetic algorithm (GA). Possible solutions are encoded on chromosomes as vectors of rate constants, which undergo cross-over and mutation. We use elite selection with elite size 20, 100 chromosomes per generation, shuffle cross-over, per-bit mutation, and a generation limit of 50. The fitness of a chromosome defined as the RNMSE reflects how well the AASP with the given rate constants (encoded in the chromosome) learns the target functions $k_1x_1 + k_2x_2 + k_0$, k_1x_1 , and k_2x_2 . The fitness of a single chromosome is then calculated as the average over 300 runs for each function. We included the k_1x_1 and k_2x_2 tasks to force the AASP to utilize and distinguish both inputs x_1 and x_2 . Otherwise the GA would have a higher tendency to opt for a greedy statistical approach where only the weight W_0 (mean) might be utilized.

4 Performance

We demonstrate the learning capabilities of the AASP on 6 linear and nonlinear target functions as shown in Table 2. During each learning iteration we inject inputs X_1 and X_2 with concentrations drawn from the interval $(0.2, 1)$ and set the bias input S_{in} concentration to 0.5. We chose the target functions carefully, such that the output concentration is always in a safe region, i.e., far from the minimal (zero) and the maximal output concentration $[S_{in}]_0 + [X_1]_0 + [X_2]_0$. We then inject the target output \hat{Y} with the learning signal S_L 50 steps after the input, which is sufficient to allow the input-weight integration to proceed.

For each function family we calculated the AASP’s performance over 10,000 simulation runs, where each run consists of 400 training iterations. We define performance as the root normalized mean square error (RNMSE)

$$\text{RNMSE} = \sqrt{\frac{\langle (y - \hat{y})^2 \rangle}{\sigma_{\hat{y}}^2}}.$$

A RNMSE of 1 means change level. The AASP’s RNMSE settles down to the range $(0.11, 0.39)$ (see Figure 3), which implies that it successfully learns and generalizes all target functions. Note that we do not distinguish between the training and testing set. During each iteration we draw the inputs with the target output for a given function independently.

Among all the functions, $k_1x_1 + k_2x_2 + k$ is the easiest (RNMSE of 0.117) and the constant function k_0 the most difficult (RNMSE of 0.388) one. The function k_0 is even more difficult than the nonlinear function $k_1x_1x_2 + k_0$ (RNMSE of 0.298). Compared to the formal perceptron, the constant function does not reach zero RNMSE because the AASP cannot fully eliminate the contribution (or consumption) of the X_1 and X_2 input-weight branches. The formal perceptron could simply discard both inputs and adjust only the bias weight, however, the AASP’s weights W_1 and W_2 with zero concentration would effectively act as inhibitors, thus consuming a part of the output produced by the bias. On the other hand, a nonlinear $k_1x_1x_2 + k_0$ function with fairly low RNMSE would be impossible to calculate for the formal perceptron. Therefore it is an open question what function classes can be learned by the AASP. Note that for the nonlinear function we set $k_0 = 0.25$, which does not increase the variance, i.e., only the nonlinear part counts toward the error. Figure 4 shows the weight concentration

Table 2: Target functions with uniform constant k_1, k_2, k_0 intervals.

\hat{y}	k_1	k_2	k_0
$k_1x_1 + k_2x_2 + k_0$	(0.2, 0.8)	(0.2, 0.8)	(0.1, 0.4)
$k_1x_1 - k_2x_2 + k_0$	(0.2, 0.8)	(0.0, 0.3)	(0.4, 0.7)
k_1x_1	(0.2, 0.8)	—	—
k_2x_2	—	(0.2, 0.8)	—
$k_1x_1x_2 + k_0$	(0.2, 0.8)	—	0.25
k_0	—	—	(0.1, 0.4)

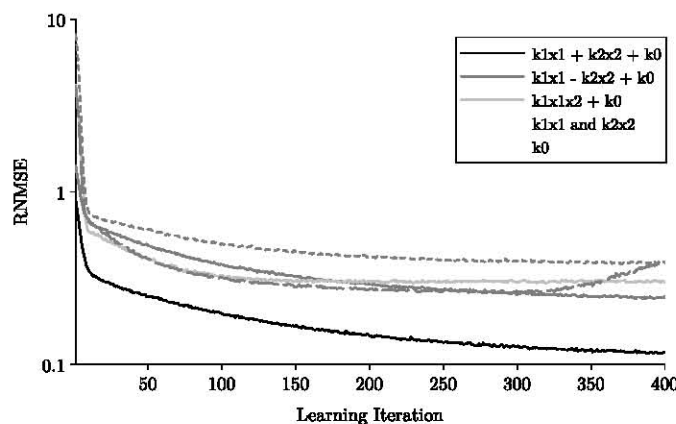


Figure 3: RNMSE for 6 linear and nonlinear functions over 400 learning iterations.

traces as well as the output, the target output, and the absolute error for selected functions.

5 Conclusion

In this paper we extended our chemical asymmetric design introduced for the asymmetric signal perceptron to an analog scenario. We demonstrated that our new AASP model can successfully learn several linear and nonlinear two-input functions. The AASP follows Michaelis-Menten and mass-action kinetics, and learns through feedback provided as a desired output.

In related work, Lakin et al. [17] designed and simulated a system based on enzymatic chemistry, capable of learning linear functions of the form $k_1x_1 + k_2x_2$. The system used more reactions (27 vs. 18) and did not reach the performance of the AASP. In addition, the AASP can learn more types of functions and the performance was evaluated more precisely over 10,000 instead of 10 trials.

Because the number of species and reactions is in the range of other state-of-the-art circuits, a wet chemical implementation, in particular using DNA-strand displacement [18, 19] and deoxyribozymes [20, 21], is within reach. As opposed to our previous designs using simple binary signals, the AASP would allow to measure and deliver medication with precise concentration levels in a smart and adaptive way. By integrating the AASP with a chemical delay line as proposed in [12], we could also tackle time-series prediction. Consequently, chemical systems would be able monitor concentrations of selected molecular species and respond if a severe event, defined as a linear or nonlinear temporal concentration pattern, occurs. Such a system would be highly relevant where the quantity or type of the drug required could be adjusted in real-time with complex relations among species, e.g., produced by cancer cells.

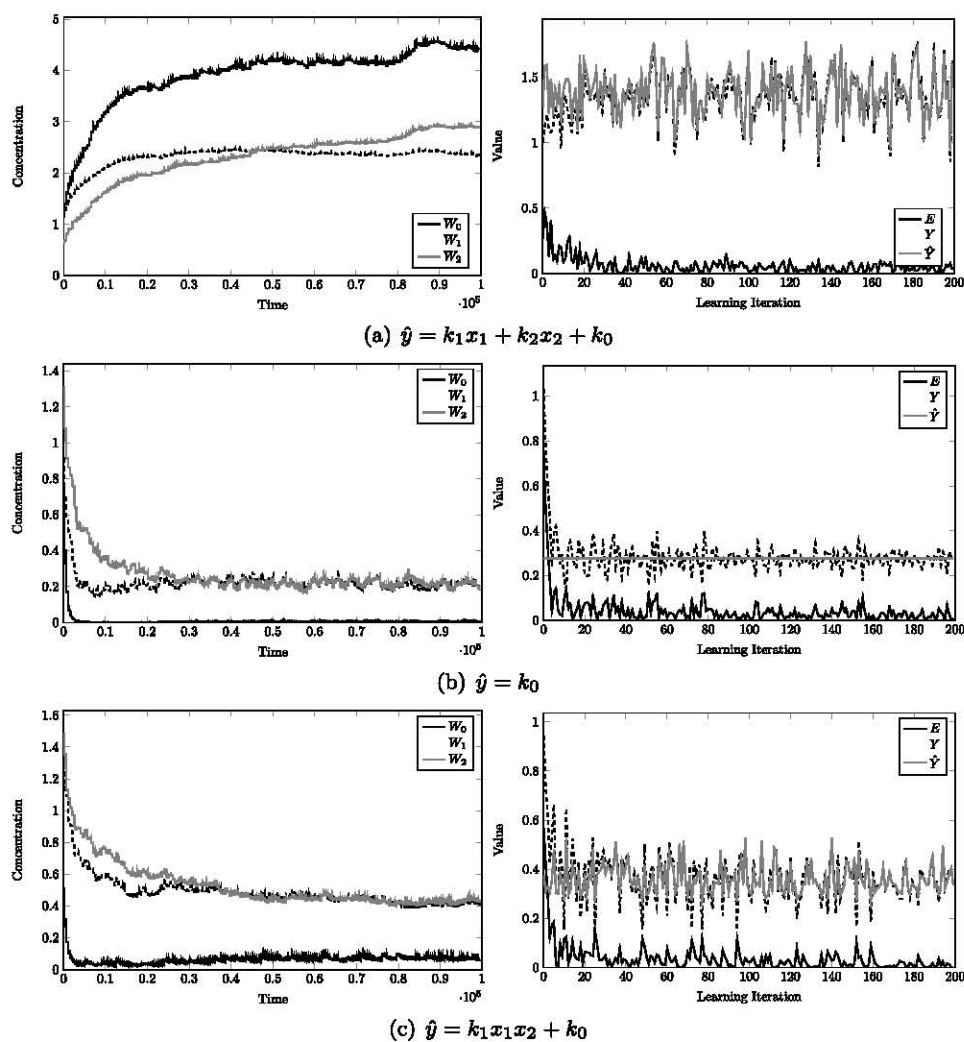


Figure 4: AASP learning examples for selected functions. The left column shows concentration traces of the weights, the right column the filtered output, the target output, and the absolute error.

Acknowledgment

This material is based upon work supported by the National Science Foundation under grant no. 1028120.

References

- [1] Wang, W., Li, S., Mair, L., Ahmed, S., Huang, T.J., Mallouk, T.E.: Acoustic Propulsion of Nanorod Motors Inside Living Cells. *Angewandte Chemie International Edition* (February 2014) n/a–n/a
- [2] Semenov, O., Olah, M.J., Stefanovic, D.: Mechanism of diffusive transport in molecular spider models. *Phys. Rev. E* **83** (Feb 2011) 021117
- [3] LaVan, D.A., McGuire, T., Langer, R.: Small-scale systems for in vivo drug delivery. *Nature biotechnology* **21**(10) (October 2003) 1184–91
- [4] Haykin, S.: *Neural networks and learning machines*. Third edn. Pearson, New Jersey (2009)
- [5] Bray, D.: Protein molecules as computational elements in living cells. *Nature* **376**(6538) (July 1995) 307–312
- [6] Mills, A.P., Yurke, B., Platzman, P.M.: Article for analog vector algebra computation. *Biosystems* **52**(1-3) (October 1999) 175–180
- [7] Kim, J., Hopfield, J.J., Winfree, E.: Neural network computation by in vitro transcriptional circuits. In Saul, L.K., Weiss, Y., Bottou, L., eds.: *Advances in Neural Information Processing Systems*. Volume 17., MIT Press (2004) 681–688
- [8] Rosenblatt, F.: The perceptron: A probabilistic model for information storage and organisation in the brain. *Psychological Review* **65** (1958) 368–408
- [9] Qian, L., Winfree, E., Bruck, J.: Neural network computation with DNA strand displacement cascades. *Nature* **475**(7356) (July 2011) 368–372
- [10] Banda, P., Teuscher, C., Lakin, M.R.: Online learning in a chemical perceptron. *Artificial life* **19**(2) (2013) 195–219
- [11] Banda, P., Teuscher, C., Stefanovic, D.: Training an asymmetric signal perceptron through reinforcement in an artificial chemistry. *Journal of The Royal Society Interface* **11**(93) (2014)
- [12] Moles, J., Banda, P., Teuscher, C.: Delay line as a chemical reaction network (under review). *Parallel Processing Letters* (2014)
- [13] Espenson, J.: *Chemical kinetics and reaction mechanisms*. McGraw-Hill, Singapore (1995)
- [14] Copeland, R.A.: *Enzymes: A practical introduction to structure, mechanism, and data analysis*. Second edn. John Wiley & Sons, Inc., New York, New York (2002)
- [15] Hornik, K., Stinchcombe, M., White, H.: Multilayer feedforward networks are universal approximators. *Neural Networks* **2**(5) (1989) 359–366

- [16] Rojas, R.: *Neural networks: A systematic introduction*. Springer-Verlag, Berlin (1996)
- [17] Lakin, M., Minnich, A., Lane, T., Stefanovic, D.: Towards a biomolecular learning machine. In Durand-Lose, J., Jonoska, N., eds.: *Unconventional Computation and Natural Computation 2012*. Volume 7445 of *Lecture Notes in Computer Science*., Springer-Verlag (2012) 152–163
- [18] Soloveichik, D., Seelig, G., Winfree, E.: DNA as a universal substrate for chemical kinetics. *Proceedings of the National Academy of Sciences of the United States of America* **107**(12) (March 2010) 5393–5398
- [19] Zhang, D.Y., Seelig, G.: Dynamic DNA nanotechnology using strand-displacement reactions. *Nature chemistry* **3**(2) (February 2011) 103–113
- [20] Stojanovic, M.N., Stefanovic, D.: A deoxyribozyme-based molecular automaton. *Nature Biotechnology* **21**(9) (August 2003) 1069–1074
- [21] Liu, J., Cao, Z., Lu, Y.: Functional nucleic acid sensors. *Chemical Reviews* **109**(5) (2009) 1948–1998 PMID: 19301873.